PD control strategy for 3 coils AMB

Adam Pilat
AGH University of Science and Technology
Department of Automatics
Al. Mickiewicza 30, 30-059Kraków, Poland
ap@agh.edu.pl

***Abstract* – This paper presents the local PD control strategy for radial Active Magnetic Bearing (AMB) designed with three electromagnets. It is the minimal configuration of actuators that allows to levitate the rotor in the electromagnetic field. The configuration of the laboratory test-rig, hardware components of the control system and description of developed algorithm is presented. Rapid prototyping environments with ability for dynamic reconfiguration that are used in the controllers design are described. The PD control algorithm as the minimal required closed loop strategy for rotor levitation is calculated and discussed to be applied in the presented control systems.**

***Index Terms* – linear and non-linear PD control, real-time control, digital and analogue control system, 3 pole AMB, rapid prototyping, embedded control system, FPGA, FPAA.**

I. Introduction

Accordingly to the author's knowledge most of radial Active Magnetic Bearings currently installed are based on four electromagnets. The electromagnets are controlled by linear and nonlinear algorithms separately, in differential configuration or using global strategy [4, 5, 6, 9, 10].

The proposed construction has three electromagnets as the necessary minimal number of actuators required for the rotor levitation in the bearing space. Less number of execution units and electronics circuits allows to minimize bearing size, production costs and energy consumption. The disadvantages of this solution correspond to the slighter stability region and strong nonlinearities. The inertia wheel based on three coils AMB was realised and is under development [1]. Development aspects of the Active Magnetic Bearing are discussed in the literature [5, 9].

II. Laboratory Test-Rig

The designed and developed laboratory test-rig is prepared to realize a wide range of research tasks. The following mechanical elements: base, radial AMB support, flexible and rigid shafts, bearing rotor, self alignment bearings, jaw coupling and unbalanced disk allows to obtain several configurations of real machines. The main goal of this laboratory test-rig is investigation of the AMB control systems and strategies in different applications. The AMB can be arranged in any place on the base to achieve the simulated configuration of the industrial device. The AMB support allows to set-up the orientation of the AMB stator every 60 degrees to obtain different configurations for research purposes. In the AMB support another configuration of AMB stator can be also installed. The mounted AMB, shaft, rotor and position sensors are shown in Fig. 1.

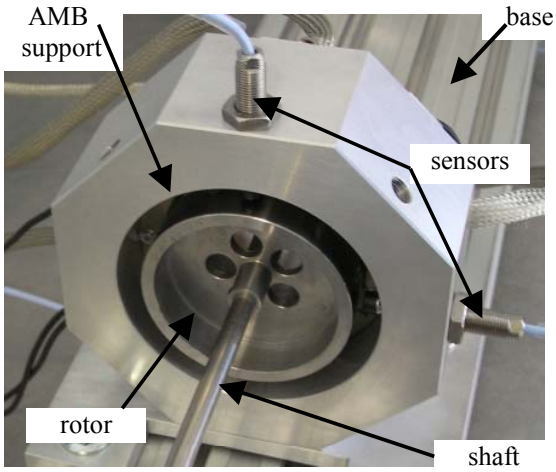

Fig. 1 Radial AMB on the test-rig

A. Three coils radial AMB

The rotor is fixed on the shaft at the desired position and placed at the bearing and sensor plane. Two proximity sensors are sensing the location of the rotor by detection of the distance between the probe and precisely prepared surface of 76mm diameter rotor track. The radial AMB air gap equals to 400μm while the rotor diameter is 51mm. The designed 25mm thick AMB stator is based on thin steel plates to eliminate eddy currents. The AMB poles and windings were designed to produce accurate forces to achieve the levitation of the 0.525kg rotor. The heteropolar construction of the AMB consists of three pole-pairs at 120 degrees apart (see Fig. 2). These three electromagnets are generating sufficient electromagnetic forces acting on the rotor for levitation and damping purposes. Three PWM power actuators are used to supply and measure coil current. For the identification purposes the system is also equipped with flux and temperature sensors. The power actuators are controlled by PWM wave with specified frequency and variable duty cycle. These control signals can be applied directly in the digital form or hardware generated using analogue reference signal.

* This work is supported by the Science Committee Research Grant #11.11.120.248 realized at Department of Automatics.

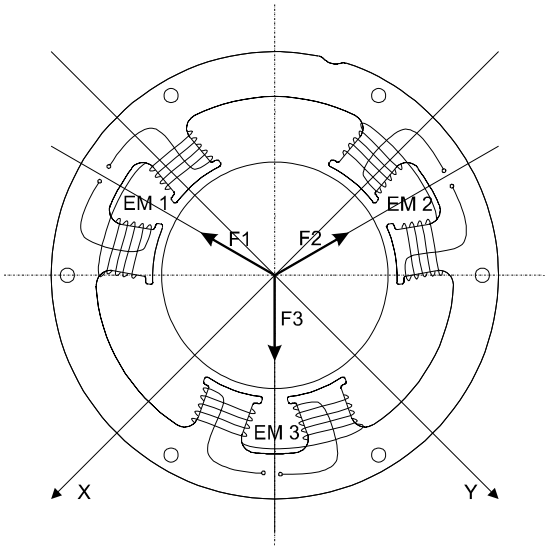

Fig. 2 General configuration of 3 coils AMB

B. Hardware and software for control purposes

To realize a wide range of control tasks few hardware and software platforms are used: PC with FPGA I/O board, 32-bit mikrocontroller and programmable analogue circuts. The common advantage of these platforms is ability of the software reconfiguration that allows to realise many custom algorithms.

On the PC platform the MATLAB/Simulink software is used to design control strategies and execute them in the real-time using Real Time Windows Target [8]. The signals flow between PC and AMB test-rig is provided by the home-made PCI control and data acquisition board. This board was accomplished using the author's experience in previous research [6].

The main advantage of this board is parallel data acquisition. This board is specially dedicated to interface MIMO systems because is able to measure up to 16 analogue signals and control up to 4 analogue interfaces.

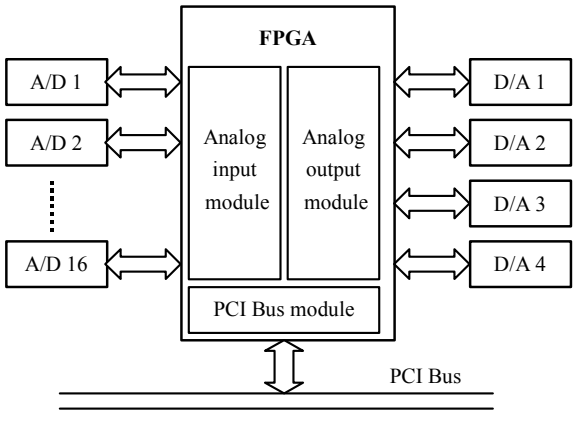

Fig. 3 Configuration of the data acquisition board

The dedicated logic is implemented in the FPGA chip to handle the communication between hardware devices. The 16 single A/D converters and 2 dual D/A converters with serial interface are connected to the FPGA unit. The internal logic controls all converters in simultaneous mode thus time delay between samples is eliminated and quality of identification and control tasks is significantly improved. In this case the disadvantages corresponding to analogue signals multiplexing are also eliminated. Another important advantage of the presented solution is that the A/D and D/A conversions are operating with maximum speed acceptable by the electronic circuits resulting in maximum sampling frequency 149kHz and 125kHz respectively. The digital form of the converted signal value is stored in the internal register of the FPGA. Also the D/A converters are handled simultaneously to apply the control signal for all channels at the same moment of time. The FPGA logic is also equipped with PCI bus interface that can exchange information via PCI bridge with the host computer via PCI bus. This interface allows to communicate the software algorithms to exchange measured and control data. The FPGA data registry scanning frequency is limited (10kHz max.) by the device-drivers using PCI bus and MATLAB/Simulink/RTWT software.

As embedded control system the MPC565 32-bit micro-controller is used. This device is characterised by PowerPC core with IEEE 754-compliant floating point unit, 1Mbyte of Flash memory, Two enhanced queued A/D converters with analogue multiplexers, modular I/O system with dedicated PWM submodules, 40MHz operation. This micro-controller can be programmed using C language and/or using the Embedded Target Toolbox for MATLAB/Simulink [3]. The implementation of algorithm elements as user defined Simulink blocks and/or c-coded s-functions allows to execute the control loop on the embedded system. Realised algorithms performs calculations using floating point data type and executing them in the FPU. Measured signals are transmitted to the host PC via serial interface using specially designed protocol and set of functions for data transfer and conversion. The realised control algorithms and math calculations are based on floating point data and are compatible for both platforms. Selection of data types and scaling formulas for math calculations must be carefully considered.

The another novel hardware configuration tested as the control system is the Field Programmable Analog Aray (FPAA) unit [7]. This reprogrammable unit allows to operate with analogue signals without conversion to the digital form. The technology of switched capacitors offers flexibility in the internal architecture design based on operational amplifiers. The FPAA device is reconfigured using the SPI interface by home made algorithm running on the host system (PC or mikrocontroller). A set of C-language functions generated from the FPAA dedicated software are used in the high level application that can perform chip configuration. This kind of application was designed to ensure the compilation for PC and PowerPC microcontroller. Thus the host control system can realise high level control and diagnosis tasks, when the hardware layer is processing analogue signals.

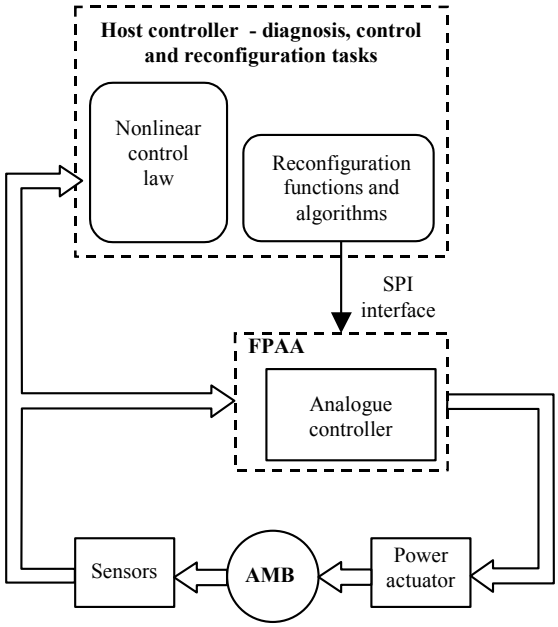

Fig. 4 Reconfigurable digital and analogue control system

The transfer of the measured and control signal generation tasks to the hardware layer allows to relieve the software layer where calculations of control signal are realised.

III. Modeling and Control

In the discussed configuration of the AMB the active flank stands 45% of the rotor surface located inside the bearing area.

A. Rotor position

For the general configuration of the AMB presented in Fig. 2. the local axial distances between the rotor and bearing poles can be calculated using trigonometric formulas based on rotor and stator dimensions, and angles between principal axes of poles and sensors.

The quality of the distance measurement is determined by the surface quality, used sensor, analog signal conditioning circuits and A/D resolution. To obtain real accuracy in the distance measurements the rotor surface was diagnosed using home-made automatic surface scanner and automatically scaled in the bearing area via custom algorithms [6]. Thus the run-out and distance scale factors were identified.

B. Selected characteristics

The identification and control tasks were realized using the host computer equipped with the presented I/O board, MATLAB/Simulink software, user defined algorithms and software components. At the identification stage the data were collected at the same moment of time for all signals.

This guarantees that all measured signals representing the physical phenomena describing static or dynamic behavior of the AMB represents its state at the particular moment of time. The values of control signals are also acquired. A wide range of static and dynamic experiments were performed to obtain the characteristics of the AMB components and to detect their manufacturing differences.

The electromagnetic force was identified using the experimental data obtained during rotor stabilization in the vertical axis at steady-state points. The experimental data and optimally approximated function are presented in Fig. 5.

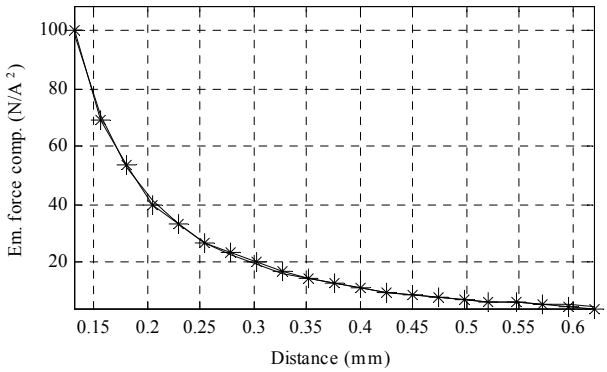

Fig. 5 Component of the electromagnetic force vs. rotor distance from electromagnet surface.

The realized identification experiment allows to obtain the electromagnetic force characteristics as the function of current and air gap volume (even the axial distance is measured). Moreover, the closed-loop identification includes properties of all control system components, thus the characteristics of the electromagnetic force is given by equation (7) with optimally tuned electromagnet constant K_{em}.

For devices equipped with analog outputs the control signal is transformed to the PWM signal characterized by fixed frequency and variable duty cycle. The realized hardware has linear characteristics in the controlled range (1). Values of all parameters used in this equation are a little bit different for every actuator.

$$d_{PWM} = \begin{cases} 0 & u \le 1 \\ au + b & 1 < u < u_{\max} \\ 1 & u \ge u_{\max} \end{cases} \quad (1)$$

In the AMB system the actuator performance is important for the control system design. The actuator dynamics can be described by the first order system (2).

$$di/dt = (k(u) \cdot u + i_{const} - i) \cdot T^{-1} \quad (2)$$

Three actuators have different constant current i_{const}, gain $k(u)$ and time-constant values T. The time constant is equal to 707μs while the actuator gain has non-linear

characteristics vs. control voltage signal u and can be approximated by the hyperbolic function (3).

$$k(u)=\begin{cases}0 & 0\le u<1\\ -a_1u^{-1}+a_2 & u\ge 1\end{cases} \tag{3}$$

In the control signal domain the dynamics of the control actuator described by (2) and (3) can be simplified to the form (6).

All mismatches in the AMB elements design should be accurately identified to obtain the real model of the system for future controller synthesis.

C. Local model

One of electromagnets of the AMB can be analyzed as the single-degree-of-freedom mass-spring-damper system [2] with controllable stiffness and damping. Using the non-contact actuator both parameters are controlled by the formulated control strategy.

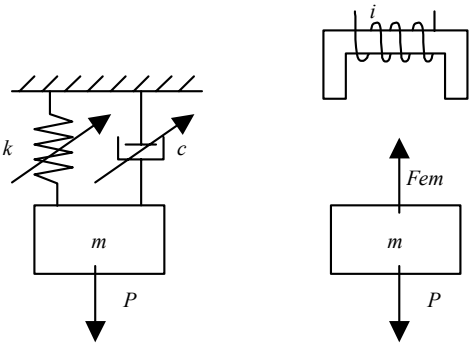

Fig. 6 Non-contact system with controllable stiffness and damping

The local nonlinear model of the electromagnetic suspension can be described by formulas (4) ÷ (6).

$$\dot{x}_1 = x_2 \tag{4}$$

$$\dot{x}_2 = m^{-1}(-F_{em}+P) \tag{5}$$

$$\dot{x}_3 = (ku + x_{3const} - x_3)T^{-1} \tag{6}$$

where: x_1 - air gap, x_2 - axial velocity, x_3 - coil current, F_{em} - electromagnetic force generated by the electromagnet, P - external force (including gravity force and force components generated by others electromagnets), u - control voltage, k - actuator gain, x_{3const} - actuator constant, T - actuator time constant.

The electromagnetic force is characterized by the following formula:

$$F_{em} = K_{em}x_3^2x_1^{-2} \tag{7}$$

For the considered AMB system there are three local models. One can notice that the P force can include gravity force and/or sum of parts ($F_{em}\sin(\pi/6)$) of electromagnetic forces generated by remaining electromagnets in the appropriate percentage contribution caused by the AMB construction – the location of electromagnets.

The steady state points depends on the rotor position and coil current. The steady state points (8) are associated with parameters chosen for every electromagnet.

$$\begin{aligned} &x_{10} = const\,,\\ &x_{20} = 0\,,\\ &x_{30} = \sqrt{Px_{10}^2K_{em}^{-1}}\,,\\ &u_0 = k^{-1}(x_{30}-x_{3const})\,. \end{aligned} \tag{8}$$

The linearized model around the operating point is given by Jacobian matrix.

$$\dot{x} = \begin{bmatrix}0 & 1 & 0\\ A_{2,1} & 0 & A_{2,3}\\ 0 & 0 & A_{3,3}\end{bmatrix}x + \begin{bmatrix}0\\0\\B_3\end{bmatrix}u \tag{9}$$

where: $A_{2,1} = 2K_{em}x_{30}^2x_{10}^{-3}m^{-1}$, $A_{2,3} = -2K_{em}x_{30}x_{10}^{-2}m^{-1}$

$A_{3,3} = -T^{-1}$, $B_3 = kT^{-1}$.

The electromagnetic force stands the main nonlinearity in the AMB system. The local linearization gives satisfactory results in the small area around the steady-state point. The nonlinear functions representing the bearing current and position stiffness shows high deviations of the electromagnetic force around the linearization point.

One can notice, that we can simplify the third order linear system to the second one. Solving the third equation of (9), for small variations of the control signal we can assume that the control signal immediately modifies the coil current. For the steady-state point we apply small control signal u around the constant control u_0 strongly associated with x_{30}. Thus we can obtain second order unstable dynamic system with direct current control. To obtain stable magnetic suspension system the PD type controller is required as the minimal feedback configuration.

D. PD controller design

Let's assume that the second order open loop system is described by (10) where α and β correspond to $A_{2,1}$ and $A_{2,3}$ respectively under above assumptions.

$$\dot{x} = \begin{bmatrix}0 & 1\\ \alpha & 0\end{bmatrix}x + \begin{bmatrix}0\\ \beta\end{bmatrix}u \tag{10}$$

The proposed PD controller (11) is stabilizing the system (10) at ($x_{10} = const, x_{20} = 0, u_0$) where u represents the coil current.

$$u(t) = -K_P x_1(t) - K_D x_2(t) \tag{11}$$

The closed loop system has two poles who can be located on the imaginary axis representing the marginally stable system but generally they are located in the left half plane to obtain desired performance. Choosing appropriate values of poles we can obtain the required dynamic behavior of the closed loop.

The obtained second order closed loop system (12) is characterized by programmable stiffness and damping settings.

$$\ddot{x} = (\alpha - \beta K_P)x - \beta K_D \dot{x} \tag{12}$$

The controller parameters K_P and K_D (13) can be designed to satisfy requirements of the closed loop performance determined by the undamped natural frequency ω_n and damping ratio ζ.

$$K_P = (\omega_n^2 + \alpha)\beta^{-1},\ K_D = 2\zeta\omega_n\beta^{-1} \tag{13}$$

Choosing the appropriate value of ω_n we can control the speed of the system response to the external disturbance. Highest natural angular frequency gives faster system response. Setting the appropriate value of damping ratio we can control the damping mode. In most cases the critically damped mode can be used because it is the most stable mode characterized by the asymptotic stability and time constant ω_n^{-1}. Note that α and β presented in the linearized system strongly depend on the selected steady-state point. Using the digital form of the PD controller the derivative component can be calculated as difference quotient. The sampling frequency affect proportionally the derivative gain of the controller. Thus the appropriate scaling factors and/or digital data lengths and data types are required for the digital controller realization.

Controller parameters depends on the selection of steady-state point. Fig. 7 and 8 shows linear variations of K_P and K_D for selected natural damping frequencies (in the critically damped mode) vs. rotor distance.

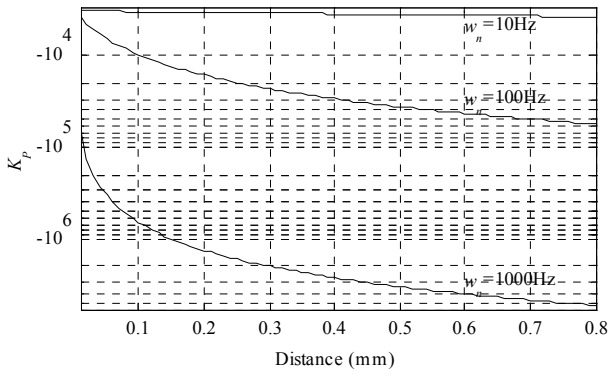

Fig. 7 Controller gain K_P vs. rotor distance

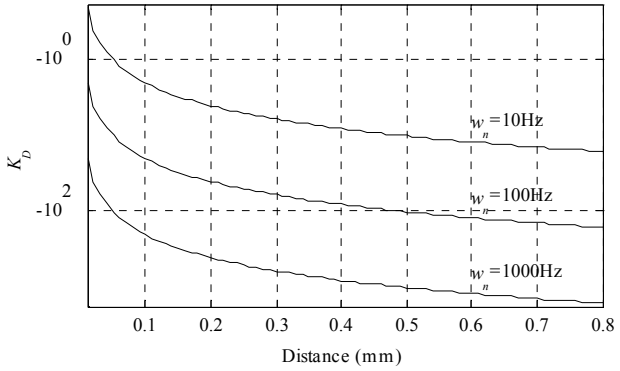

Fig. 8 Controller gain K_D vs. rotor distance

For the tracking trajectory applications when the desired performance of the closed loop is required the PD controller must be reprogrammed for every steady-state point.

Changing the maximum force acting on the rotor at steady-state point via appropriate current value the parameters of the controller ought to be redesigned. For the rotor stabilization at the bearing center the actuator force increased up to 80N (16 times bigger than gravity one). The nonlinear variation of controllers parameters is observed (see Fig. 9 and Fig. 10).

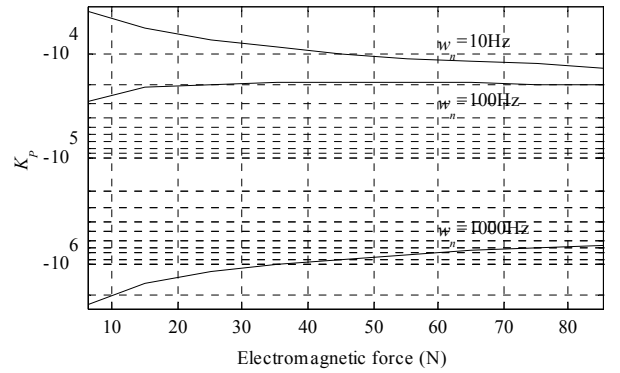

Fig. 9 Controller gain K_P vs. electromagnetic force

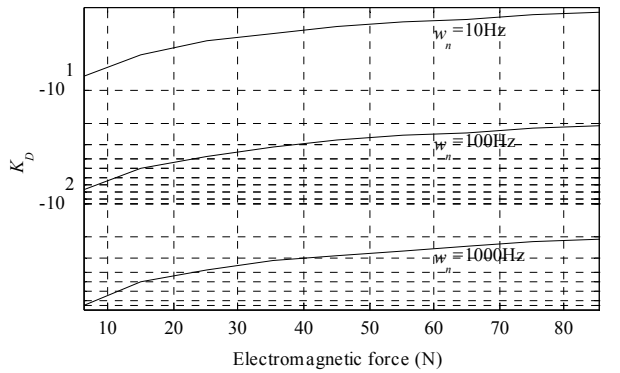

Fig. 10 Controller gain K_D vs. electromagnetic force

For the small electromagnetic forces the influence of the rotor mass is high and the bearing robustness for external forces is small.

To check the sensitivity of the designed controller the eigenvalues of the closed loop system were calculated for rotor displacement disturbances. For the selected operating steady-state point corresponding to the rotor center and for selected natural frequency $\omega_n = 10\text{Hz}$ and damping ratio $\zeta = 1$ the PD controller gains were calculated. The system was linearized in few rotor displacements around the steady-state point and the designed controller was applied. The location of eigenvalues (see Fig. 11) correspond to rotor displacements. The performance of the closed loop was changed too.

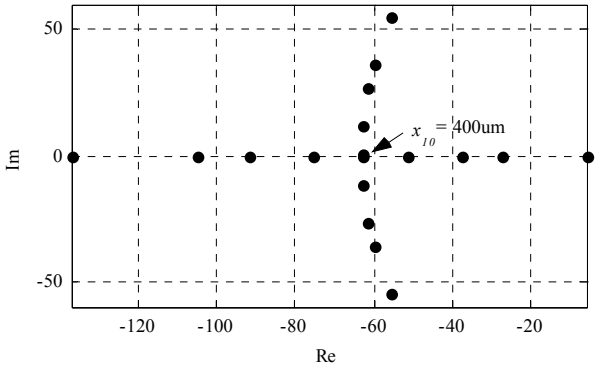

Fig. 11 Eigenvalues of the closed-loop system for rotor displacement around bearing center

IV. Experiments

Using the designed PD controller the rotor was suspended at the bearing centre (see Fig. 12). Three local PD controllers were calculating the control in the real-time with 10kHz sampling frequency. In the controller design the rotor mass was considered.

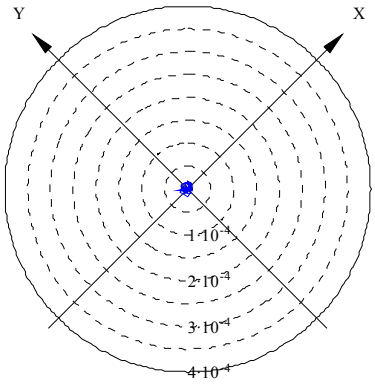

Fig. 12 Rotor stabilization at the bearing center

V. Future research

Future research will be focussed on quality comparison between presented hardware and software platforms. During the controller design it is important to take into considerations hardware and software performance. The analogue signal and digital data processing strongly influences on the control quality. The hardware current controller will be realized to move the coil current stabilization task to the hardware layer. The global control strategy including rotary motion will be compared to the local form using digital control tools.

V. Conclusions

The synthesis of the local PD controllers for three coils AMB requires precise identification and modeling of actuators and electromagnetic force. The manufacturing mismatches must be also considered.

Three local PD controller allows to stabilize the rotor in three coils AMB, but their parameters should be carefully designed.

The application of the PD controller allows to choose the stiffness and damping performance of every magnetic suspension in the AMB. Because of the variable form of the controller parameters, the control algorithm requires the ability to programmable reconfiguration of the direct control loop to achieve desired feedback performance.

The application of simultaneous sampling home made I/O board was the most important part in the identification and control research. This solution allows to eliminate time-delays in the data processing and proceed with maximum speed limited by the hardware and real-time software performance.

The application of the dedicated software and hardware architectures allows to design and execute in the real-time mode the control application with proposed control algorithm.

The analyzed control strategy can be applied in any controlled magnetic suspension system.

References

[1] Chiaberge M., Damilano C., Maddaleno F., Genta G. FPGA Based Transconductance Amplifier for AMB Application, ISCORMA-2, August 4-8, 2003, Gdansk, Poland.

[2] Clarence de W.Silva, Vibration Fundamentals and Practice, CRC Press 2000.

[3] Embedded Target for Motorola MPC555 User's Guide, MathWorks, Inc. 2002.

[4] Gosiewski Z., Falkowski K, Multifunctional magnetic bearings (in Polish), BNIL, Warsaw 2003.

[5] Maslen E.: Magnetic Bearings. University of Virginia, Department of Mechanical, Aerospace and Nuclear Engineering, Charlottesville, Virginia, 1999.

[6] Piłat A., Control of Magnetic Levitation Systems, Ph.D. Thesis, AGH University of Science and Technology, Cracow, Poland, 2002 (in Polish).

[7] Piłat A., Programmable analog hardware for control systems exampled by magnetic suspension, Computer Methods and Systems, November 14-16, 2005, Cracow, Poland, pp. 143–148.

[8] Real-Time Windows Target User's Guide, MathWorks, Inc. 1999

[9] Schweitzer G., Traxler A. Bleuler H.: *Magnetlager.* Springer-Verlag, 1994.

[10] Proceeding of 9th International Symposium on Magnetic Bearings, August 3-6, 2004 , Lexington, Kentucky, USA.